ACEEE Int. J. on Electrical and Power Engineering , Vol. 5, No. 1, February 2014

Design and Performance Analysis of Genetic based PID-PSS with SVC in a Multi-machine System Considering Detailed Model

Hitesh Rameshchandra Jariwala[1] and Anandita Chowdhury [2]
[1] Electrical Engineering Department, S. V. National Institute of Technology, Surat, 395007, India.
Email: hrj@svnit.ac.in
[2] Electrical Engineering Department, S. V. National Institute of Technology, Surat, 395007, India.
Email: ac@svnit.ac.in

Abstract— **Damping of power system oscillations with the help of proposed optimal Proportional Integral Derivative Power System Stabilizer (PID-PSS) and Static Var Compensator (SVC)-based controllers are thoroughly investigated in this paper. This study presents robust tuning of PID-PSS and SVC-based controllers using Genetic Algorithms (GA) in multi machine power systems by considering detailed model of the generators (model 1.1). The effectiveness of FACTS-based controllers in general and SVC-based controller in particular depends upon their proper location. Modal controllability and observability are used to locate SVC–based controller. The performance of the proposed controllers is compared with conventional lead-lag power system stabilizer (CPSS) and demonstrated on 10 machines, 39 bus New England test system. Simulation studies show that the proposed genetic based PID-PSS with SVC based controller provides better performance.**

Index Terms— **Controllability, Genetic algorithms, Observability, Power system modeling, Static VAr compensators.**

NOMENCLATURE

δ	Generator rotor angle
ω	Generator rotor speed
M	Generator moment of Inertia
ϕ	Angle of bus voltage
I	Magnitude of line current
I_R	Shunt injected reactive current
V	Magnitude of bus voltage
P_{sh}	Shunt injected real power
Q_{sh}	Shunt injected reactive power
B_{sh}	Shunt injected susceptance

I. INTRODUCTION

Damping of power system oscillations between interconnected areas is very important for the reliable and secured system operation. Such oscillations are of low frequency (0.5 Hz -3 Hz) and occur when there is a fault in the system or sudden change in load [1-2] or when existing generation/load areas are connected to other similar areas through relatively weak transmission lines.

With the increase in the demand it is very common that power is transferred from one area to another through a tie line. These oscillations may enforce limitations on power transfer through tie line and/or may be responsible for loss of synchronism. The damping of electromechanical oscillations can be achieved by means of a proper control strategy. The use of a supplementary control added to the Automatic Voltage Regulator (AVR) is a practical and economic way to supply additional damping to electromechanical oscillations and it is achieved with the help of Power System Stabilizer (PSS).

The widely used conventional power system stabilizer (CPSS), basically a lead-lag compensator, is designed using the theory of phase compensation in the frequency domain considering deviation of speed as control signal. It is important to note that the parameters of the machine change with loading. The dynamic behavior of the machine is quite different with different operating conditions. A set of PSS parameters which give good system performance under a certain operating condition may not give equally good result under different operating conditions. Sometimes CPSS may cause great variation in the voltage profile and may even result in leading power factor operation under severe disturbances [3]. In order to improve the performance of CPSS, quite good numbers of tuning techniques such as optimal control, adaptive control, variable structure control etc. have been proposed [4]. Apart from the techniques mentioned above, methods based on artificial intelligence techniques such as GA, simulated annealing, tabu search, fuzzy logic, partical swam optimization etc. are also used for obtaining parameters of CPSS [3-6].

Apart from PSSs, Flexible AC Transmission Systems (FACTS) devices are also used to improve system stability. Particularly, in multi-machine systems, use of CPSS may not provide sufficient damping for inter-area oscillations. In such cases, FACTS devices can provide effective damping [1-2], [5-7]. Although, the damping duty of FACTS devices is not their primary function, the capability of FACTS based controller to increase electromechanical damping characteristics has been recognized. The FACTS devices are capable enough to control network conditions in a very fast manner and this feature of FACTS can be exploited to improve system stability [8]. FACTS devices such as Static VAr Compensators (SVC), Static Synchronous Compensators (STATCOM), Thyristor Control Series Compensators (TCSC) and Unified Power Flow Controller (UPFC) have led their use

DOI: 01.IJEPE.5.1.6

to damp inter-area oscillations [7-10].

Unlike PSS control at a generator location, the speed deviations of the machines of interest are not readily available to FACTS devices sited in the transmission path. Furthermore, speed signals themselves may not be the best choice for an input signal for FACTS devices. Because of these reasons, it is desired to extract an input signal from the locally measurable quantities at the controller location [11-12]. An SVC is usually located at mid-point of a transmission line or near the loads if voltage control is required. The location is not so obvious when SVC is required for damping purpose. Most of the studies suggest the midpoint of a transmission line or load buses as the location for SVCs as the voltage swings are maximum at these locations. Others however, propose the generator bus bar for placing SVCs to damp oscillations. In some studies, the location of SVC is found using residue method. There obviously exists difference of opinion for the best location of a SVC for damping of low frequency oscillations.

Various techniques were applied to improve the performance of the controllers. M. A. Abido *et al.* [7], [13-14] have discussed the enhancement of stability by designing PSS and SVC using real coded genetic algorithms considering change in rotor speed as input for both controllers and Single Machine Infinite Bus (SMIB) system was considered. Hu Guo-qiang *et al.* [15] have used GA to design PSS for a four machine system and verified its performance under different operating conditions. Khodabakhshian *et al.* have [5] applied same concept for a multi-machine system. Y. L. Abdel-Magid *et al.* [16] applied TABU search method to tune parameters of PSS for multi-machine system in which synchronous machines are represented by model 1.0. Li-Jun Cai *et al.* [1] applied Sequential Quadratic Programming (SQP) algorithm for simultaneous tuning of PSS and FACTS damping controllers in large power systems. X. Y. Bian *et al.* [17] have employed probabilistic eigenvalue-based objective function for design of PSS and SVC. Ahad Kazemi *et al.* [18] applied fuzzy logic to tune parameters of PSS and FACTS based controllers. A. Andreoiu *et al.* [19] have applied a Lyapunov method based GA to tune the parameters of PSS and applied it to SMIB system.

In most of the studies, change in rotor speed is considered as input signal to SVC controller and generators were represented by model 1.0. The objective of this study is to present use of proposed PID-PSS controller and SVC based controller for damping of power system oscillations with locally available signals in multi-machine systems in which all generators are represented by their detailed model (model 1.1). The optimal setting of parameters of both proposed PID-PSS and SVC controller is obtained using Genetic algorithms. The location of PID-PSS can be determined with the help of Participation Factors [2]. However, in this study, it is considered that all machines are equipped with proposed PID-PSS.

To locate shunt FACTS devices like SVC, modal analysis is carried out as discussed in the section II [11]. Modal controllability and observability are determined for locally available signals. Controllability of a signal depends on location and nature of the FACTS device under consideration. A higher controllability of a signal means smaller variable compensation requirement of a controller.

The modal observability based ranking of candidate locations can be more convenient than modal controllability or residue based ranking as it can be done a priori on a system without explicitly representing the FACTS damping controller at each candidate location.

II. Modal Analysis of Power Systems

In order to identify the best location to site SVC and to determine control signals for SVC based controller, linearized analysis is carried out in which synchronous machine is represented by its classical model. The controllability-observability relationship for various locally available signals is determined in this section.

A. Modal Analysis

For a multi-machine interconnected power system, the complex non-linear model can be described in a set of differential-algebraic equations by assembling the models for each generator, load and other devices such as controls in the system, and connecting them appropriately via the network algebraic equations. These differential-algebraic equations of a non-linear power system are given as,

$$\begin{aligned} \Delta\dot{X} &= A\Delta X + Bu \\ Y &= C\Delta X + Du \end{aligned} \tag{1}$$

Classical techniques for the analysis and design of controllers are mostly based on the linearized representation of the power system at a representative operating point. While carrying out linearized analysis of power system, following assumptions are made:

1. Loads are considered as constant impedance type.
2. Synchronous machines are represented by classical model.
3. Mechanical input to the generator is considered as constant.
4. FACTS devices are considered as fast acting devices as compared to the period associated with power swings.

The linearized swing equations along with the real and reactive power balance equations for all nodes and the lines in which shunt and series compensation is present can be represented as follows [2], [11].

$$\begin{bmatrix} \Delta\dot{\delta} \\ -M\Delta\dot{\omega} \\ \Delta P_{sh} \\ \Delta I_R \end{bmatrix} = J \begin{bmatrix} \Delta\delta \\ \Delta\omega \\ \Delta\phi \\ \Delta V \end{bmatrix} \tag{2}$$

where, matrix J is represented as follows:

DOI: 01.IJEPE.5.1.6

$$J = \begin{bmatrix} [0] & I & [0] & [0] \\ A_{11} & [0] & A_{12} & A_{13} \\ A_{21} & [0] & A_{22} & A_{23} \\ A_{31} & [0] & A_{32} & A_{33} \end{bmatrix} \quad (3)$$

Here A_{ij} are block matrices, M is a diagonal matrix and following relationship holds true for the block matrices of J.

$$A_{ij} = A_{ji}^T \quad i, j = 1\ldots 3 \quad (4)$$

The elements of various sub-matrices shown in (3) are the partial differentiations of (5) to (8) with respect to variables mentioned in (2). For the k^{th} generator, the swing equation can be expressed as;

$$M_k \frac{d^2\delta_k}{dt^2} = P_{mk} - P_{ek} \quad k = 1,2,\ldots n_g \quad (5)$$

where, n_g is number of generators in the system.

At any bus j (except generator internal bus), the injected power P_{shj} by a FACTS controller is given by;

$$P_{shj} = P_{Lj} + \sum_{i\in n_j} \frac{V_j V_i}{x_{ij}} \sin\left(\phi_j - \phi_i\right) + \sum_{k\in m_j} \frac{V_j E_k}{x'_{dk}} \sin\left(\phi_j - \phi_k\right) \quad (6)$$

where, n_j is set of buses connected to bus j by a transmission line, m_j is the set of generator (internal) buses connected to bus j. P_{Lj} is the power consumed by the load connected at bus j, x_{ij} is the reactance of the transmission line connecting bus i and j and x'_{dk} is the transient reactance of generator k. At the k^{th} generator internal bus, injected power is given by,

$$P_{ek} = \frac{E_k V_j}{x'_{dk}} \sin\left(\delta_k - \phi_j\right) \quad (7)$$

The reactive current balance equation at the j^{th} node is given by:

$$I_{Rj} = -V_j b_{shj} + \sum_{i\in n_j} \frac{V_j}{x_{ij}} - \frac{V_i \cos\left(\phi_j - \phi_i\right)}{x_{ij}} + \sum_{k\in m_j} \frac{V_j}{x'_{dk}} - \frac{V_j \cos\left(\delta_j - \phi_k\right)}{x'_{dk}} \quad (8)$$

where, b_{shj} is the fixed shunt susceptance at j^{th} bus.

The controllable inputs of the system are:

$$u = \left[\Delta P_{sh}^T \quad \Delta I_R^T\right]^T \quad (9)$$

while observable quantities of the system are:

$$y = \left[\Delta\phi^T \quad \Delta V^T\right]^T \quad (10)$$

Equation (2) can be written in state space form as follows;

$$\begin{bmatrix} \Delta\dot{\delta} \\ \Delta\dot{\omega} \end{bmatrix} = A \begin{bmatrix} \Delta\delta \\ \Delta\omega \end{bmatrix} + Bu \quad (11)$$

$$y = C \begin{bmatrix} \Delta\delta \\ \Delta\omega \end{bmatrix} + Du \quad (12)$$

$$A = \begin{bmatrix} [0] & I \\ -M^{-1}A_r & [0] \end{bmatrix} \quad (13)$$

$$A_r = A_{11} - \begin{bmatrix} A_{12} & A_{13} \end{bmatrix} J_r \begin{bmatrix} A_{21} \\ A_{31} \end{bmatrix} \quad (14)$$

$$B = M^{-1} \begin{bmatrix} [0] & [0] \\ A_{12} & A_{13} \end{bmatrix} J_r \quad (15)$$

$$C = -J_r \begin{bmatrix} A_{21} & [0] \\ A_{31} & [0] \end{bmatrix} \quad (16)$$

$$J_r = \begin{bmatrix} A_{22} & A_{23} \\ A_{32} & A_{33} \end{bmatrix}^{-1} = D \quad (17)$$

B. Modal Controllability and Observability

There is one eigenvector associated with each eigenvalue of the state matrix A. For the i^{th}-eigenvalue $\ddot{e}_i$, the eigenvector e_i satisfies the equation.

$$\lambda_i e_i = A e_i = A \begin{bmatrix} e_{\delta i} \\ e_{\omega i} \end{bmatrix} \quad (18)$$

Each right eigenvector is a column vector with length equal to number of states. The left eigenvector f_i satisfies the equation

$$f_i^T \lambda_i = f_i^T A = \begin{bmatrix} f_{\delta i}^T & f_{\omega i}^T \end{bmatrix} A \quad (19)$$

For the system under consideration, it can be verified that the right and left eigenvectors of state matrix A corresponding to i^{th} eigenvalue λ_i have the following form:

$$e_i = \begin{bmatrix} e_{\delta i} \\ e_{\omega i} \end{bmatrix} = \begin{bmatrix} e_{\delta i} \\ \lambda_i e_{\delta i} \end{bmatrix} \quad (20)$$

$$f_i = \begin{bmatrix} f_{\delta i} \\ f_{\omega i} \end{bmatrix} = \begin{bmatrix} \lambda_i f_{\omega i} \\ f_{\omega i} \end{bmatrix} \quad (21)$$

Due to symmetry of the state matrix A and A_r, the left and right eigenvectors are related with each other as follows:

$$f_i = k_i \begin{bmatrix} \lambda_i M e_{\delta i} \\ M e_{\delta i} \end{bmatrix} \quad (22)$$

Here, k_i is a constant whose value can be chosen arbitrarily.

The modal controllability and observability vectors are defined by (23) and (24) respectively.

$$\beta_i = \left(f_i^T B\right)^T = B^T f_i \quad (23)$$

$$\gamma_i = C e_i \quad (24)$$

From (13) to (24), it can be shown that,

$$\beta_i = k_i \gamma_i \quad (25)$$

Above relation suggests that modal controllability and observability vectors are parallel. This relation shows that relative modal controllability using various inputs mentioned in u can be inferred from the relative modal observability in

DOI: 01.IJEPE.5.1.6

the output signals mentioned in *y*. Hence, the location of series or shunt FACTS devices can be determined using modal observability of the mode in the appropriate local signals.

The structure and symmetry of the sub-matrices A_{ij} unchanged if the inputs and corresponding outputs are

$$u' = \left[\Delta P_{sh}^T \quad \Delta Q_{sh}^T\right]^T \tag{26}$$

$$y' = \left[\Delta\phi^T \quad \Delta V^T / V_o\right]^T \tag{27}$$

or

$$u'' = \left[\Delta P_{sh}^T \quad \Delta B_{sh}^T\right]^T \tag{28}$$

$$y'' = \left[\Delta\phi^T \quad V_o \Delta V^T\right]^T \tag{29}$$

Same results can be obtained for these set of inputs and outputs. In this study, input-output pairs corresponding to shunt FACTS devices are only considered. Here, V_o is initial operating voltage.

III. Controllers

The low frequency oscillations can be damped with the help of controllers. In this study, a comparison is made on the performance of CPSS, PID-PSS and SVC based controllers. The structure of these controllers is as discussed below.

A. Conventional PSS

PSS introduces a component of additional damping torque proportional to speed change through the excitation system. The standard IEEE type-1 excitation system is as shown in Fig.1(a). The structure of CPSS is illustrated in Fig 1(b). It consists of an amplification block, a wash out block and a lead/lag block. The lead-lag blocks provide required phase compensation. The input signal to the CPSS can be change in speed, change in power or can be the combination of both. In this study, change in speed of a machine is considered as input to the CPSS.

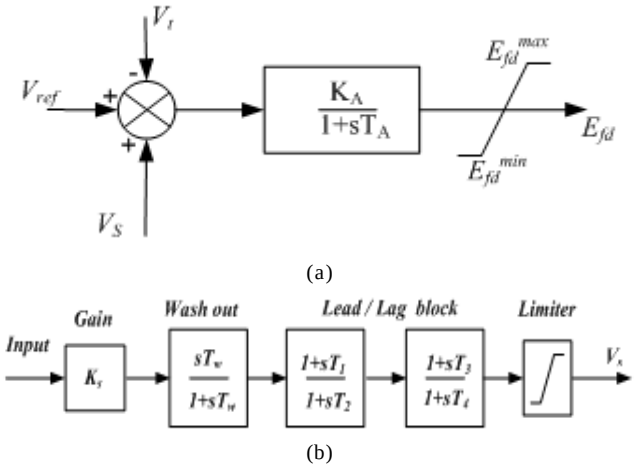

Figure 1. (a) Excitation system (b) Conventional PSS

B. Proposed PID-PSS

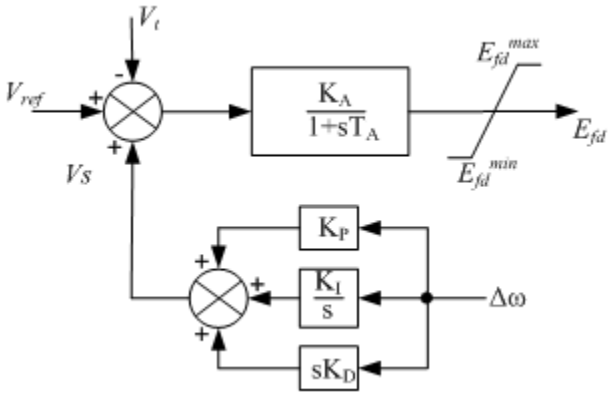

Figure 2. Structure of PID-PSS with excitation system

The structure of PID-PSS along with excitation system is as shown in Fig.2. The input to the PID-PSS controller is change in rotor speed ($\Delta\omega$) of the machine on which it is installed. The system can be described.

$$\text{as. } \frac{dE_{fd}}{dt} = \frac{1}{T_A}\left(K_A\left(V_{ref} - V_t + V_s\right)\right) \tag{30}$$

where, K_A and T_A are the gain and time constant of the excitation system respectively; V_{ref} is the reference voltage; K_P, K_I and K_D are the Proportional, Integral and Derivative gain for the machine on which it is installed. The supplementary stabilizing signal V_s is generated with the help of PID-PSS installed in the feedback loop is as shown in Fig. 2.

C. SVC Based Controller

Figure 3 represents the block diagram of a SVC with lead-lag compensator [3]. The susceptance *B* of an SVC can be expressed as:

$$\frac{dB_{sh}}{dt} = \frac{1}{T_s}\left(K_s\left(B_{ref} - u_{svc}\right) - B_{sh}\right) \tag{31}$$

where, B_{ref} is the reference susceptance of SVC, K_s and T_s are gain and time constant of SVC respectively.

The parameters of CPSS are obtained using phase compensation techniques and those of PID-PSS and SVC based controller are obtained with the help of GA, which is discussed in next section.

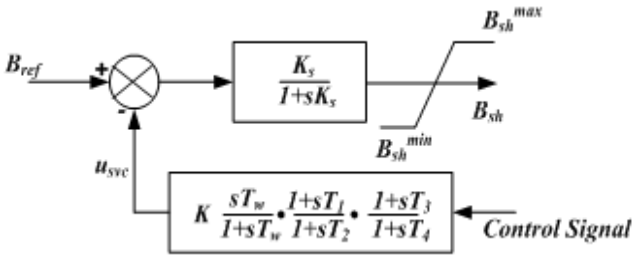

Figure 3. SVC based controller

IV. Objective Function and GA

GA have recently found extensive applications in solving global optimization searching problems. They are useful when

DOI: 01.IJEPE.5.1.6

the closed form optimization technique cannot be applied. GA simultaneously evaluates many points in the parameter space, so it is more likely to converge towards global minimum solution.

GA is used to search for optimal PID controller parameters. GA are powerful search algorithms based on the mechanics of natural selection and natural genetics.

- These algorithms work with a population of strings, searching many peaks in parallel, as opposed to a single point.
- GA work directly on strings of characters representing the parameter set, not the parameter themselves.
- GA use probabilistic transition rules instead of deterministic rules.
- GA use objective function information instead of derivatives or other auxiliary knowledge.

To determine the optimal controller settings, GA method is applied. GA optimal technique is used to minimize performance index which is of Integral Square Error (ISE) type.

Objective function considered is,

$$\text{Minimize } J_e = \int_0^\infty e^2(t)dt \qquad (32)$$

To get the optimal setting of K_P, K_I and K_D, the error function is minimized.

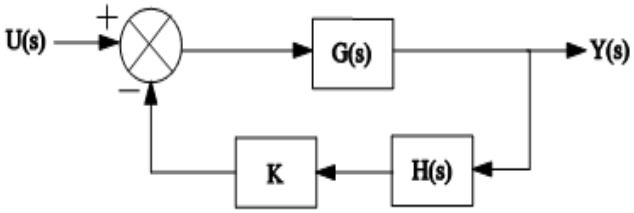

Figure 4. Transfer function

Here, *e(t)* is the error signal generated by taking a difference between reference input and the feedback signal as shown in Fig 4. In this study, speed deviation (*Äù*) of individual machine is considered as error function while designing proposed PID-PSS.

V. Simulation Results

To validate the discussion done in previous sections, simulation is carried out on the 10 machine, 39 bus system as shown in Fig.5. The system data and the load flow data are taken from [20]. The generators are represented by a classical model and loads are modeled as constant impedance. This system has nine oscillatory modes with eigenvalues as shown in Table I.

The magnitude of controllability and observability are obtained by considering shunt susceptance B_{sh} as an input and bus voltage V as an output of the system for the swing mode ($ë = 0.0004896 \pm 4.2432i$) having frequency 0.6756 Hz. These values are mentioned in Table II which shows that the ratio of controllability to observability is constant for the input-output pair mentioned above. These results suggest that modal controllability and modal observability vectors are parallel. The normalized values of above quantities show that susceptance of bus no. 4 has the highest controllability. The voltage of same bus number has the highest observability. So, the observability vector alone can be used to locate shunt FACTS device like SVC.

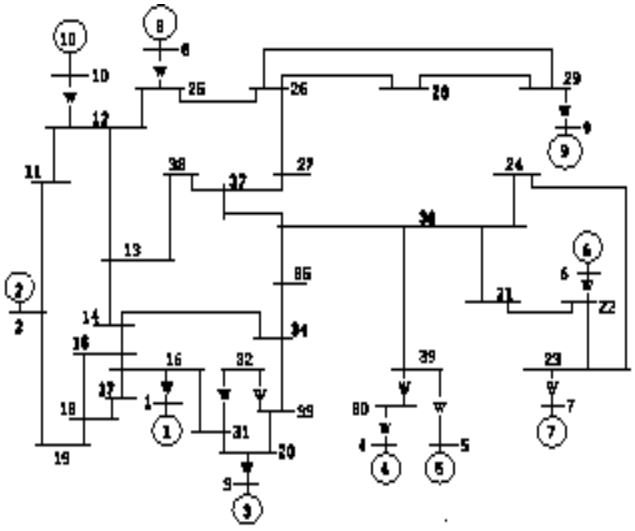

Figure 5. 10 machines, 39 bus test system

Table I. Oscillatory Modes - Classical Model

Sr. no.	Eigenvalues corresponding to oscillatory modes
1	$0.0005898 \pm 9.4268i$
2	$0.0004152 \pm 9.7135i$
3	$0.0004109 \pm 9.7847i$
4	$0.0005942 \pm 8.1050i$
5	$0.0007225 \pm 7.7813i$
6	$0.0001917 \pm 7.6271i$
7	$0.0002408 \pm 6.8163i$
8	$0.0004412 \pm 6.2298i$
9	$0.0004896 \pm 4.2432i$

The values of controllability and observability considering B_{sh} as an input and bus voltage V as an output of the system are also obtained considering detailed model of the generators (model 1.1). In this case also the loads are modeled as constant impedance. There are nine swing modes for the system under consideration and the eigenvalues corresponding to these modes are as listed in Table III (eigenvalues without controllers). The real parts of these eigenvalues suggest that the damping is very poor and system may become unstable if a disturbance is applied as two of the eigenvalues have positive real part. The magnitudes of controllability and observability are shown in Table IV for a swing mode ($l = -0.085428 \pm 4.3617i$) having frequency of 0.6943 Hz and damping ratio of 0.0196. In this case the ratio of controllability to observability does not remain constant but remains in a narrow range. A closer scrutiny of Table II and Table IV show that ranking of locations by observability vector for the classical and detailed model matches closely. The bus with highest controllability and highest observability is the same and it agrees with the result obtained with classical model of the generators. Hence, observability vector alone can be used to screen out locations with poor controllability.

DOI: 01.IJEPE.5.1.6

TABLE II. CONTROLLABILITY AND OBSERVABILITY-CLASSICAL MODEL

	λ= -0.085428 ± 4.3617i				
Bus no.	β	γ	$\frac{\beta}{\gamma}$	$\frac{\beta}{\beta_{max}}$	$\frac{\gamma}{\gamma_{max}}$
1	2.6662	0.005263	506.56	0.50381	0.50381
2	2.0464	0.00404	506.54	0.38669	0.38671
3	3.1599	0.006238	506.56	0.59712	0.59712
4	**5.292**	**0.010447**	**506.56**	**1**	**1**
5	5.0363	0.009942	506.56	0.95168	0.95168
6	5.0392	0.009948	506.56	0.95223	0.95222
7	5.2187	0.010302	506.57	0.98615	0.98614
8	3.0389	0.005999	506.56	0.57424	0.57424
9	4.8879	0.009649	506.57	0.92365	0.92362
10	2.6766	0.005284	506.55	0.50579	0.5058
11	0.37291	0.000736	506.52	0.070466	0.070472
12	2.4218	0.004781	506.55	0.45763	0.45764
13	2.7303	0.00539	506.54	0.51593	0.51596
14	2.5239	0.004983	506.53	0.47694	0.47696
15	2.2057	0.004355	506.54	0.41681	0.41683
16	2.2466	0.004435	506.54	0.42452	0.42454
17	1.9057	0.003762	506.53	0.3601	0.36012
18	1.7505	0.003456	506.53	0.33078	0.3308
19	0.56084	0.001107	506.54	0.10598	0.10598
20	2.6755	0.005282	506.55	0.50557	0.50558
21	4.2277	0.008346	506.55	0.79889	0.79891
22	4.6403	0.009161	506.56	0.87686	0.87687
23	4.6413	0.009163	506.56	0.87705	0.87705
24	3.9509	0.0078	506.54	0.74658	0.7466
25	2.7169	0.005364	506.55	0.51339	0.5134
26	3.4477	0.006806	506.54	0.65149	0.65151
27	3.4311	0.006774	506.54	0.64835	0.64838
28	4.0542	0.008004	506.55	0.76611	0.76612
29	4.3129	0.008514	506.56	0.81499	0.81498
30	4.8738	0.009622	506.55	0.92098	0.92099
31	2.5331	0.005001	506.54	0.47867	0.47868
32	2.6192	0.005171	506.54	0.49494	0.49495
33	2.7104	0.005351	506.54	0.51216	0.51218
34	2.8122	0.005552	506.54	0.53142	0.53144
35	3.5124	0.006934	506.54	0.66372	0.66375
36	3.8622	0.007625	506.54	0.72981	0.72984
37	3.4934	0.006897	506.54	0.66014	0.66016
38	3.1883	0.006294	506.54	0.60248	0.6025
39	4.6738	0.009227	506.55	0.88319	0.8832

TABLE III. OSCILLATORY MODES WITHOUT AND WITH CONTROLLERS-DETAILED MODEL

Sr. no.	Eigen values without controllers	Eigen values with controllers
1	-0.04820 ± 10.3350i	-0.2892 ± 9.2470i
2	-0.17342 ± 10.2740i	-0.3087 ± 9.7690i
3	0.09861 ± 9.9508i	-0.2767 ± 9.1052i
4	-0.25513 ± 8.8299i	-0.7190 ± 8.3784i
5	- 0.29057 ± 7.6048i	-0.7806 ± 7.4287i
6	-0.38441 ± 8.1870i	-1.2647 ± 7.9450i
7	0.07293 ± 7.5473i	-0.2432 ± 7.4274i
8	-0.00586± 8.3051i	-0.2365 ± 8.1529i
9	-0.08542 ± 4.3617i	-0.3642 ± 4.1705i

VI. DESIGN OF CONTROLLERS

A. Design of PID-PSS

To determine the parameters of PID-PSS of each machine, the optimization problem is formulated as below:

Minimize J_e

Subject to

TABLE IV. CONTROLLABILITY AND OBSERVABILITY-DETAILED MODEL

	λ= -0.085428 ± 4.3617i				
Bus no.	β	γ	$\frac{\beta}{\gamma}$	$\frac{\beta}{\beta_{max}}$	$\frac{\gamma}{\gamma_{max}}$
1	0.46134	0.038352	12.029	0.51711	0.5255
2	0.30674	0.025051	12.244	0.34381	0.34326
3	0.52266	0.04355	12.001	0.58584	0.59672
4	**0.89216**	**0.072982**	**12.224**	**1**	**1**
5	0.84201	0.069044	12.195	0.94379	0.94604
6	0.84818	0.068945	12.302	0.95071	0.94469
7	0.86773	0.0707	12.273	0.97262	0.96874
8	0.51707	0.042497	12.167	0.57957	0.5823
9	0.72616	0.060394	12.024	0.81394	0.82752
10	0.48531	0.039818	12.188	0.54397	0.54559
11	0.04693	0.003975	11.808	0.052609	0.054465
12	0.4427	0.036444	12.148	0.49621	0.49935
13	0.49356	0.041727	11.828	0.55322	0.57174
14	0.46066	0.039276	11.729	0.51634	0.53817
15	0.40939	0.034459	11.88	0.45887	0.47216
16	0.41587	0.034794	11.952	0.46613	0.47675
17	0.36049	0.03079	11.708	0.40406	0.42188
18	0.33449	0.028768	11.627	0.37492	0.39418
19	0.07020	0.005251	13.371	0.07869	0.071944
20	0.48174	0.039751	12.119	0.53997	0.54467
21	0.74473	0.061158	12.177	0.83475	0.838
22	0.80583	0.065218	12.356	0.90323	0.89362
23	0.80633	0.065368	12.335	0.90379	0.89567
24	0.69747	0.058152	11.994	0.78177	0.7968
25	0.48684	0.039964	12.182	0.54569	0.54759
26	0.59805	0.049684	12.037	0.67034	0.68078
27	0.60078	0.050714	11.846	0.6734	0.69488
28	0.6747	0.055217	12.219	0.75626	0.75659
29	0.69933	0.05695	12.28	0.78386	0.78034
30	0.85037	0.069054	12.315	0.95316	0.94618
31	0.46035	0.038129	12.074	0.51599	0.52244
32	0.47464	0.039325	12.07	0.53202	0.53883
33	0.4892	0.04052	12.073	0.54833	0.55521
34	0.50811	0.042596	11.929	0.56953	0.58365
35	0.62359	0.052608	11.853	0.69897	0.72084
36	0.68261	0.056884	12	0.76512	0.77943
37	0.61813	0.051943	11.9	0.69285	0.71173
38	0.56775	0.048025	11.822	0.63637	0.65805
39	0.81197	0.065928	12.316	0.91012	0.90334

$$\begin{aligned} K_P^{\min} \le K_P \le K_P^{\max} \\ K_I^{\min} \le K_I \le K_I^{\max} \\ K_D^{\min} \le K_D \le K_D^{\max} \end{aligned} \tag{33}$$

where J_e is the objective function mentioned in (32).

The parameters of PID-PSS are obtained by following an algorithm as shown in Fig. 6. To set the optimal values of parameters of proposed PID-PSS, GA has been applied with moderate population size of 20, number of generation 20, small mutation probability of 0.002 and relatively high cross over probability 0.8.

The convergence graph of performance index for generator 5 is shown in Fig 7. It shows that PI decreases with increase in number of generations and it is converging after 10 generations. Similarly the parameters of other PID-PSS installed on respective machine are obtained. The final settings of the optimized parameters for the proposed stabilizer are given in Table V.

DOI: 01.IJEPE.5.1.6

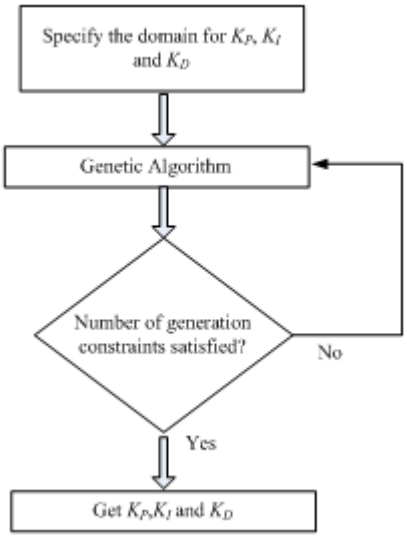

Figure 6. Flow chart to design PID-PSS based on GA

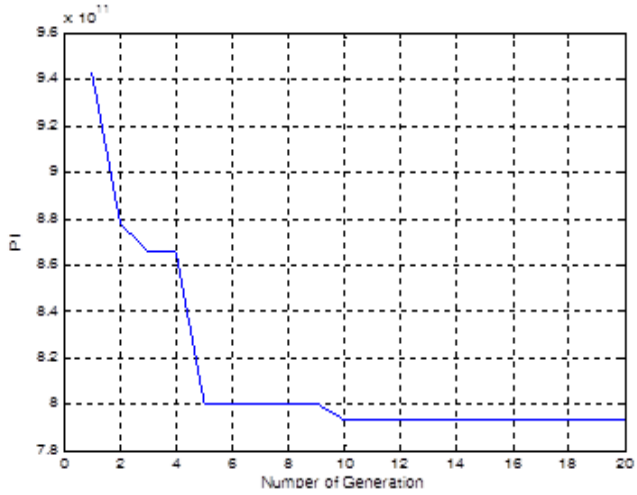

Figure 7. Convergence graph of performance index for PID-PSS

TABLE V. OPTIMAL PARAMETERS OF PID-PSS

Generator	K_P	K_I	K_D
1	93.3058	88.949	1.3914
2	98.5082	94.9153	0.0457
3	81.1264	80.0	4.2767
4	82.8837	83.678	1.408
5	80.2594	88.6323	1.3914
6	80.2594	89.8823	1.0202
7	82.9365	80.457	5.8136
8	80.7004	86.8653	5.4705
9	80.7003	82.4903	1.408
10	86.6681	91.3689	1.1093

B. Design of SVC Based Controller

The parameters of the SVC based controller are obtained by solving following optimization problem using GA. In this controller, T_w, T_2 and T_4 are usually pre-specified [3].

Minimize J_e

Subject to

$$K^{\min} \le K \le K^{\max}$$
$$T_1^{\min} \le T_1 \le T_1^{\max} \quad (34)$$
$$T_3^{\min} \le T_3 \le T_3^{\max}$$

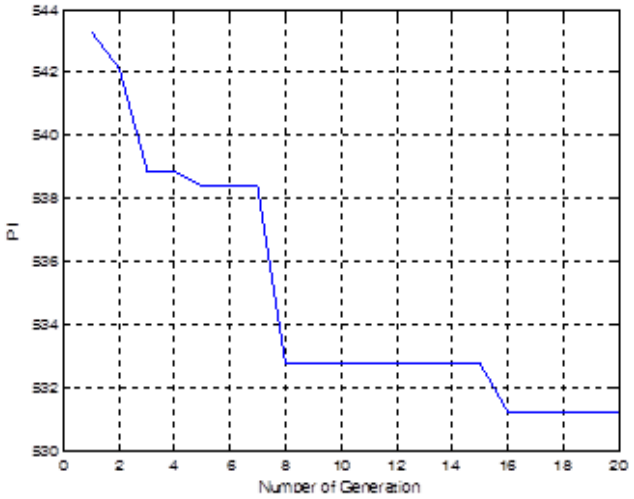

Figure 8. Convergence graph of performance index for SVC

To set the optimal values of parameters of SVC, GA has been applied with moderate population size of 50, number of generation 20, small mutation probability of 0.005 and relatively high cross over probability 0.4. The convergence graph of performance index (PI) is shown in Fig. 8. In this case also PI decreases with increase in number of generations and it is converging after 16 generations. The optimum parameters of SVC based controller are obtained by following the algorithm mentioned in Fig. 6 in which K_P, K_I and K_D are replaced by K, T_1 and T_3 respectively and they are mentioned in Table VI.

TABLE VI. OPTIMAL PARAMETERS OF SVC BASED CONTROLLER

K	T_1	T_2	T_3	T_4
3	0.2248	0.1945	0.2323	0.3484

The location of the SVC based controller is determined by studying modal controllability and observability of the susceptance signal B_{sh} and bus voltage V respectively. The values of controllability and observability mentioned in Table IV suggest that bus no. 4 is the best location for SVC to damp power system oscillations. The voltage of bus no. 4 is considered as the control signal for the controller. To compare the performance of proposed PID-PSS and SVC based controllers, CPSSs are also designed for each machine. The parameters of the CPSS are obtained by using phase compensation techniques and they are listed in Table VII.

To verify the performance of the controllers, a 200 ms three phase fault (10 cycles) is created on bus no. 14 of the test system. In order to observe full transient behavior of the system, sufficiently large simulation time is considered. The variation of rotor angle of generator 1 and generator 3 are shown in Fig. 9 and Fig. 10, respectively for aforesaid fault.

The performance is also verified by increasing the fault duration to 300 ms (15 cycles) at the same location. The variation of rotor angle of generator 1 and generator 3 are shown in Fig. 11 and Fig. 12, respectively for this fault duration. It is found that settling time for the responses considering CPSS is about 20 s. It is improved to about 10 s when machines are equipped with proposed PID-PSS. The settling time is less

DOI: 01.IJEPE.5.1.6

TABLE VII. PARAMETERS OF CPSS

Generator	T_W	K	T_1	T_2	T_3	T_4
1	10	8	0.1699	0.0122	0.0932	0.1695
2	10	9	0.52	0.004	0.0875	0.1179
3	10	9	0.487	0.0038	-	-
4	10	7	0.512	0.0034	0.2477	0.0826
5	10	7	0.512	0.0034	0.2477	0.0826
6	10	8	0.52	0.004	-	-
7	10	2	0.03977	0.5195	0.03977	0.5195
8	10	2	0.03977	0.5195	0.03977	0.5195
9	10	7	0.512	0.0034	0.2477	0.0826
10	10	7	0.512	0.0034	0.2477	0.0826

than 10 s when proposed PID-PSSs act along with SVC. The peak deviations are also reduced when proposed PID-PSSs act along with SVC.

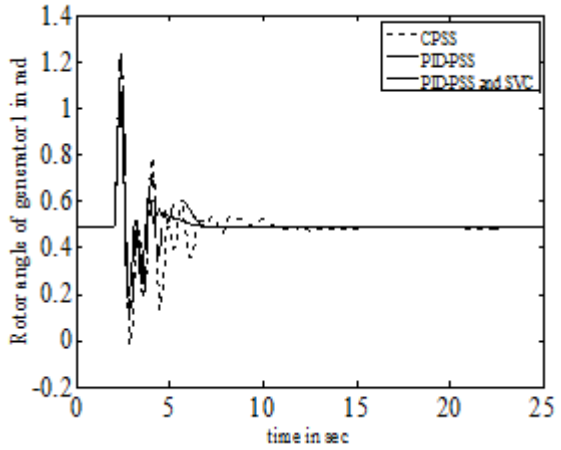

Figure 9. Rotor angle of generator-1 for a fault on bus no.14 for 0.2s

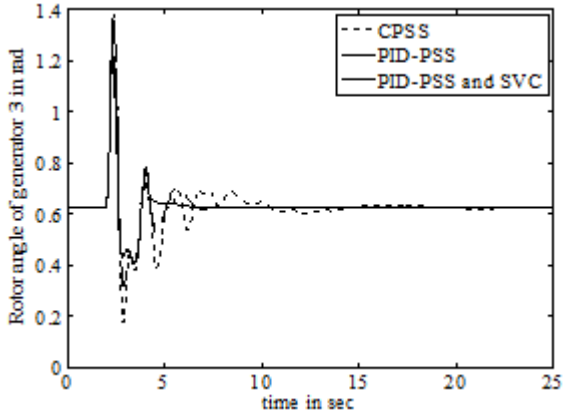

Figure 10. Rotor angle of generator -3 for a fault on bus no.14 for 0.2s

To check robustness of the controllers, a step change of 0.2 pu is applied to mechanical power input to generator 1. The oscillations in rotor angle of generator 1 due to this change are shown in Fig.13. In this case overshoots are almost vanished when PID-PSSs are used. In this case also the result is further improved when proposed PID-PSS and SVC controllers act together and generator reaches to its new angular position quickly as compared to CPSS. Similar results can be obtained for other generators and any other fault location.

The eigenvalues corresponding to swing modes are

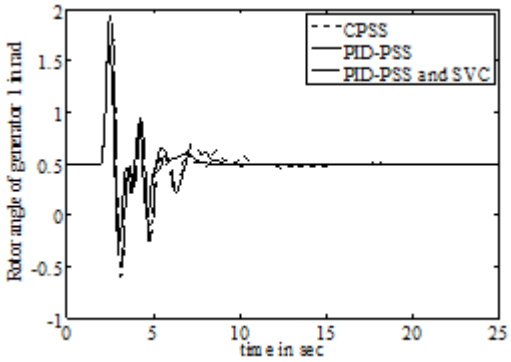

Figure 11. Rotor angle of generator-1 for a fault on bus no.14 for 0.3s

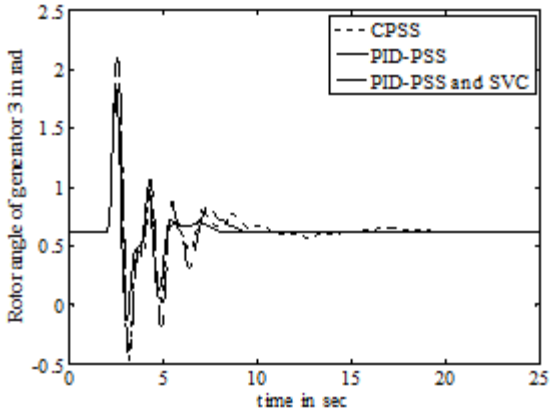

Figure 12. Rotor angle of generator -3 for a fault on bus no.14 for 0.3 s

mentioned in Table III without controllers and with proposed PID-PSSs and SVC based controller. The eigenvalues corresponding to swing modes with controllers are as shown in Table III (eigenvalues with controllers). The improvement in the real part of eigenvalues is the indication of the good performance of the controllers.

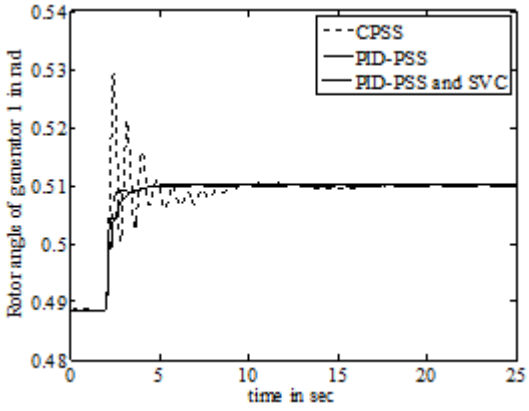

Figure 13. Rotor angle of generator-1 for a change of 0.3 pu in mechanical input of generator 1

VII. CONCLUSIONS

The power system stability enhancement with the help of proposed PID-PSS and SVC-based controllers is presented and discussed. The GA optimal technique was used to find optimal setting of PID-PSS and SVC-based stabilizers. Modal

DOI: 01.IJEPE.5.1.6

controllability vector and observability vectors are parallel for certain input-output pairs when generators are represented by classical model. Hence, modal observability vector can be used to locate FACTS devices. The ratio of these vectors is not constant when detailed model (model-1.1) of the generator is considered. However, the ratio remains within the narrow range for certain input-output pairs as mentioned and ranking based on classical model and detailed model match closely. Hence, the modal observability can be used to screen out locations with poor controllability.

The location of SVC and its control signal are determined by modal analysis. The proposed GA based stabilizers were tested on a multi-machine power system by applying various disturbances. The simulation results show the robustness and effectiveness of the suggested stabilizers to enhance the system stability. The results are also compared with conventional lag-lead type PSS with change in speed as an input to stabilizer. The simulation results show that the proposed PID-PSSs give better results than conventional PSSs. The use of SVC-based stabilizer improves the performance of the system further.

References

[1] Li-Jun Cai, Istvan Erlich, "Simultaneous coordinated tuning of PSS and FACTS damping controllers in large power systems", IEEE Trans. on Power Systems, vol.20, No.1, pp. 294-299 February 2005.

[2] Magdy E. Aboul-Ela, A. A. Sallam, James D. McCalley, A. A. Fouad, "Damping controller design for power system oscillations using global signals ", IEEE Trans. on Power Systems, vol.11, No.2, pp. 767-773, May 1996.

[3] Pouyan Pourbeik, Michael J. Gibbard, "Simultaneous coordination pf power system stabilizers and FACTS devices stabilizers in a multimachine power system for enhancing dynamic performance", IEEE Trans on Power Systems, vol. 13, No.2, pp.473-478, May 1998.

[4] Ning Yang, Qinghua, James D. McCalley, "TCSC controller design for damping inter area oscillations", IEEE Trans on Power Systems, vol.13, No 4, pp1304-1310, November 1998.

[5] A. Khodabakhian, R. Hooshmand, R. Sharifian, "Power system stability enhancement by designing PSS and SVC parameters coordinately using RCGA", Canadian Conf. on Electrical and Computer Engineering, pp.579-582, 2009.

[6] Nadarajah Mithulananthan, Claudio A. Canizares, John Reeve, Graham J. Rogers, "Comparison of PSS, SVC and STATCOM controllers for damping power system oscillations", IEEE Trans. on Power Systems, vol.18, no.2, pp1-6, May 2003.

[7] M. A. Abido, Y. L. Abdel-Magid, "Power system stability enhancement via coordinated designs of a PSS and an SVC based controller", 10th IEEE conf. on Electronics, Circuits and Systems, pp. 850-853, 2003.

[8] Y. L. Abdel-Majid, M. A. Abido, S. Al-Baiyat, A. H. Mantawy, "Simultaneous stabilization of multi-machine power systems via genetic algorithms", IEEE Trans. PWRS, Vol. 14, No. 4, pp.1428-1439, 1999.

[9] Y. L. Abdel-Majid, M. A. Abido, "Optimal multi-objective design of robust power system stabilizers using genetic algorithms", IEEE Tran. on Power systems, vol. 18, No. 3, pp. 1125-1132, August 2003.

[10] A. Beik Khormizi, A. Salem Nia, "Damping of power system oscillations in multi-machine power systems using coordinate design of PSS and TCSC", 10th international conference on Environment and Electrical Engg., pp.1-4, 2011.

[11] U. P. Mhaskar, A. M. Kulkarni, "Power oscillation damping using FACTS devices: Modal controllability. Observability in local signals and location of transfer function zeros", IEEE Trans. on Power Systems, vol. 21, No.1, pp. 285-294 February 2006.

[12] Suman Bhowmick, "A comparison of commonly used signals for power oscillations damping", 1st IEEE Indian annual conference, pp.456-459, 2004.

[13] M. A. Abido, "Design of PSS and STATCOM based damping stabilizers using genetic algorithms", IEEE Power Engineering Society General Meeting, pp.1-8, 2006.

[14] M. A. Abido, Y. L. Abdel-Magid, "Coordinated design of a PSS and an SVC based controller to enhance power system stability", Elsevier journal on Elect. Power and Energy Sys., vol. 25, pp. 695-704, 2003.

[15] H. Guo-qiang, X. Dong-jie, H. Ren-mu, "Genetic algorithms based design of power system stabilizers", IEEE conf. on Electric utility, Deregulation, Restructuring and Power Tech., 167-171, April 2004.

[16] Y. L. Abdel-Magid, M. A. Abido, A. H. Mantawy, "Robust tuning of power system stabilizers in multi-machine power systems", IEEE Trans. on Power Systems, vol.15, No.2, pp 735-740 May 2000.

[17] X. Y. Bian, C. T. Tse, J.F. Zhang, K. W. Wang, "Coordinated design of probabilistic PSS and SVC damping controllers", Elsevier journal on Electrical Power and Energy Systems, vol. 33, pp. 445-452, 2011.

[18] Ahad Kazemi, Mahmoud Vakili Sohrforouzani, "Power system damping using fuzzy controlled facts devices", Elsevier journal on Electrical Power and Energy Systems, vol. 28, pp. 349-357, 2006.

[19] A. Andreoiu, K. Bhattacharya, "Robust tuning of power system stabilizers using a Lyapunov method based genetic algorithms", IEE Proceedings on Generation, Transmission and Distribution, vol.149,No.5, pp.585-592, September 2002.

[20] A. K. Behra, "Transient stability analysis of multi-machine power systems using detailed machine models", Ph. D Thesis, University of Illinois, Urbana-Champaign, 1988.

DOI: 01.IJEPE.5.1.6